

A neuron–astrocyte transistor-like model for neuromorphic dressed neurons

G. Valenza^{a,b,*}, G. Pioggia^c, A. Armato^{a,b}, M. Ferro^d, E.P. Scilingo^{a,b}, D. De Rossi^{a,b}

^a Department of Information Engineering, University of Pisa, Italy

^b Interdepartmental Research Center “E. Piaggio”, University of Pisa, Italy

^c National Research Council of Italy (CNR), Institute of Clinical Physiology (IFC), Pisa, Italy

^d National Research Council of Italy (CNR), Institute of Computational Linguistics “A. Zampolli” (ILC), Pisa, Italy

ARTICLE INFO

Article history:

Received 10 February 2010

Received in revised form 4 March 2011

Accepted 8 March 2011

Keywords:

Neuron

Astrocyte

Synapse

Neuron–astrocyte interaction model

ABSTRACT

Experimental evidences on the role of the synaptic glia as an active partner together with the bold synapse in neuronal signaling and dynamics of neural tissue strongly suggest to investigate on a more realistic neuron–glia model for better understanding human brain processing. Among the glial cells, the astrocytes play a crucial role in the tripartite synapse, i.e. the dressed neuron. A well-known two-way astrocyte–neuron interaction can be found in the literature, completely revising the purely supportive role for the glia. The aim of this study is to provide a computationally efficient model for neuron–glia interaction. The neuron–glia interactions were simulated by implementing the Li–Rinzel model for an astrocyte and the Izhikevich model for a neuron. Assuming the dressed neuron dynamics similar to the nonlinear input–output characteristics of a bipolar junction transistor, we derived our computationally efficient model. This model may represent the fundamental computational unit for the development of real-time artificial neuron–glia networks opening new perspectives in pattern recognition systems and in brain neurophysiology.

© 2011 Elsevier Ltd. All rights reserved.

1. Introduction

Traditionally, astrocytes have been considered to be non-excitable cells of the brain able to provide only structural and metabolic support to the neurons. However, in the last twenty years, this view has been changing. In fact, the large amount of experimental data characterizing the communication processes between astrocytes and astrocyte–neurons showed the possible role of glial cells in the dynamics of neural tissue. These recent results on the active functional role of the synaptic glia cells together with synapses in neuronal signaling (Fellin & Carmignoto, 2004; Newman, 2003; Nobile, Monaldi, Alloiso, Cugnoli, & Ferroni, 2003; Parpura et al., 1994; Parpura & Haydon, 2000) propose new approaches to applied neuroscience. Investigations on a neuron–glia alternative for the basis of human brain information processing are currently developing (Volman, Ben-Jacob, & Levine, 2007).

From a physiological point of view, astrocytes regulate the synaptic signaling current between two neurons modulating the amount of neurotransmitters into the synaptic cleft through inter-

and intracellular calcium dynamics (Di Garbo, Barbi, Chillemi, Alloiso, & Nobile, 2007; Newman, 2003; Parpura & Haydon, 2000; Volman et al., 2007). In detail, calcium dynamics is controlled by the interplay of calcium-induced calcium release, a nonlinear amplification method triggering the modulation of the pre-synaptic and post-synaptic neural activities and promoting depolarizing currents in neurons (De Pitta, Goldberg, Volman, Berry, & Ben-Jacob, 2009; Volman et al., 2007). The interplay of calcium-induced calcium release nonlinear amplification method is dependent on calcium channels opening to calcium stores such as the endoplasmic reticulum, and the action of active transporters that enable a reverse flux (De Pitta et al., 2009; De Pitta' et al., 2008; Volman et al., 2007). The level of inositol 1, 4, 5-trisphosphate is directly controlled by signals impinging on the cell from its external environment. The elevation of the intracellular calcium level in astrocytes, promoted by the extracellular glutamate, triggers the release of glutamate from the astrocyte, modulating the pre-synaptic and post-synaptic depolarizing currents in neurons. Furthermore, inositol 1, 4, 5-trisphosphate dynamics are encoded by nonlinear amplitude and frequency modulation phenomena, while calcium oscillations are inherently frequency modulated (De Pitta' et al., 2008).

Concerning derived nonlinear models, there are no extensive mathematical studies on dynamics of neuron–glia interactions, and the first systematic attempts to build a self-consistent model of the tripartite synapse in order to seize its dynamical and computational properties are under development (Allegrini, Fronzoni,

* Corresponding author at: Department of Information Engineering, University of Pisa, Italy.

E-mail addresses: g.valenza@iet.unipi.it (G. Valenza), giovanni.pioggia@ifc.cnr.it (G. Pioggia), antonino.armato@centropiaggio.unipi.it (A. Armato), marcello.ferro@ilc.cnr.it (M. Ferro), e.scilingo@centropiaggio.unipi.it (E.P. Scilingo), d.derossi@centropiaggio.unipi.it (D. De Rossi).

Pirino & Pirino, 2009; De Pitta' et al., 2008; Di Garbo et al., 2007; Volman et al., 2007). Regarding single neurons, the most accurate biophysical model has been developed by Hodgkin and Huxley (Hodgkin & Huxley, 1952), following the so-called Hodgkin and Huxley Model (HHM). This model is able to exactly reproduce the shape of an action potential taking into account the involved ionic currents. The HHM is onerous to be implemented since it requires about 1200 FLOPs to simulate one millisecond of a single neuron activity. Several models attempt to reduce the mathematical complexity of such a neuron model, i.e. the Morris–Lecar model (Morris & Lecar, 1981) takes about 600 FLOPs, while the FitzHugh–Nagumo model (FitzHugh, 1961) takes about 72 FLOPs for one millisecond of neuron activity.

Izhikevich recently developed a simple model for an artificial neuron (Izhikevich, 2003, 2004). This model is able to reproduce several functionalities of a biological neuron. It takes 13 FLOPs to emulate one millisecond of neuron activity. Regarding astrocytes, the Li–Rinzel (LR) model has been used to describe calcium dynamics (Li & Rinzel, 1994; Nadkarni & Jung, 2004). Considering a minimal neural network model made up of two coupled units, a neuron and an astrocyte, (the so-called “dressed” neuron), we can adopt the mathematical formulation for the neuron–glia signaling according to Nadkarni and Jung (Nadkarni & Jung, 2004, 2003). These authors showed how the astrocyte is critical for the generation of firing activity of the neuron. More complete models, including plasma membrane calcium fluxes, suggest several differences compared to the model obtained by these authors (Di Garbo et al., 2007).

From an engineering point of view, this behavior resembles the functionalities of a Bipolar Junction Transistor (BJT), where the collector–emitter current can be viewed as being controlled by the base–emitter current. A transistor-like model for the neuron–astrocyte information processes could open new dramatic perspectives in neuroscience and neuroengineering, as well as in modern electronics. In this work we demonstrate how the dressed neuron signaling can be formalized through a transistor-like transfer function, starting from evidences in experimental data obtained by Nadkarni and Jung model (Nadkarni & Jung, 2004, 2003). Future processing architectures can be organized around bi-dimensional grids of such an interacting artificial dressed neuron.

2. Experimental and biophysical models of tripartite synapses

The tripartite (three-part) synapse involves: a pre-synaptic neuron releasing neurotransmitters (glutamate) which activates or inhibits the activity of a post-synaptic neuron, the post-synaptic neuron and the astrocyte which protects cells by taking up glutamate to prevent overexcitation and secretes growth factors (Newman, 2003; Parpura et al., 1994; Parpura & Haydon, 2000; Volman et al., 2007). The astrocyte provides energy via glucose and modulates receptors function by locally released neurotransmitters. Regarding the pre-synaptic neuron, we can adopt the artificial neuron model proposed by Izhikevich (Izhikevich, 2007). It consists of several parameters, two equations and one condition:

$$\begin{cases} C v' = k(v - v_r)(v - v_t) - u + I_n \\ u' = a[b(v - v_r) - u] \end{cases} \quad (1)$$

with the condition:

$$\text{if } v \geq v_{\text{peak}}, \text{ then } \begin{cases} v \leftarrow c \\ u \leftarrow u + d. \end{cases} \quad (2)$$

The v variable represents the membrane potential of the pre-synaptic neuron, while u , a recovery current, keeps into account the activation and deactivation of ionic currents. C is the membrane capacitance, v_r is the resting membrane potential and v_t is the

Table 1

The model parameters for RS neurons.

C	100 pF	a	0.03
k	0.7	b	−2
v_r	−60 mV	c	−50 mV
v_t	−40 mV	d	100
v_{peak}	35 mV		

instantaneous threshold potential. k and b can be found knowing the neuron's rheobase and the input resistance. The sum of all slow currents that modulate the spike-generation mechanism is combined in the phenomenological mechanism and in the phenomenological variable u . The I_n variable takes into account the synaptic currents and the bias currents as the input signal of the neuron. All these parameters can easily fit the six fundamental classes of firing patterns observed in the mammalian neocortex (Izhikevich, 2007). Even if most of the biologists agree with this classification, the distinction between the six classes is not sharp; some subclasses within each class and neurons can change their firing classes depending on the state of the brain.

Regular Spiking (RS) neurons are the major class of excitatory neurons in the neocortex. They fire tonic spikes with adapting (decreasing) frequency in response to injected pulses of dc-current. The interspike frequency vanishes as the amplitude of the injected current decreases. Morphologically, RS neurons are spiny stellate cells in layer 4 and pyramidal cells in layers 2, 3, 5, and 6. The model parameters for the RS neurons are reported in Table 1. In the case of a modulation coming from an astrocyte, the model can be modified as:

$$\begin{cases} C v' = k(v - v_r)(v - v_t) - u + I_n + I_{\text{astro}} \\ u' = a[b(v - v_r) - u] \end{cases} \quad (3)$$

with the same condition. I_{astro} represents the contribution of the astrocyte in terms of modulation current toward the post-synaptic neuron.

Astrocyte processes are in close contact with neuronal synapse. They are accurate sensors of neuronal activity and respond to the synaptic release of glutamate with oscillations in the intracellular calcium concentration. Glutamate elevations in astrocyte domain trigger the internal release of inositol 1, 4, 5-trisphosphate (IP3) which stimulates intracellular calcium dynamics. The properties of intracellular calcium oscillations generated in astrocytes, including their amplitude, frequency and propagation, are governed by the intrinsic properties of both neuronal inputs and astrocytes. Astrocytes discriminate neuronal inputs of different origins, and can integrate concomitant inputs responding to calcium elevations. Calcium dynamics is controlled by the interplay of calcium-induced calcium release, i.e. a nonlinear amplification method depending on the calcium channels opening to calcium stores, such as the endoplasmic reticulum (ER). The action of active transporters (SERCA pumps) enables a reverse flux (see Fig. 1). The level of IP3 is directly controlled by signals impinging on the cell from its external environment. In turn, the level of IP3 determines the dynamical behavior of the LR model. One can therefore consider the calcium signal as an encoded information regarding the level of IP3. In detail, by varying two key parameters of the model, the information can be encoded in amplitude or in frequency modulations of the calcium levels (Fellin & Carmignoto, 2004; Nobile et al., 2003; Volman et al., 2007). These findings were recently demonstrated by De Pitta' et al. (2008). The elevation of the intracellular calcium level in astrocytes, promoted by the extracellular glutamate, triggers the release of glutamate from the astrocyte modulating the pre-synaptic and post-synaptic neural activities by promoting a depolarizing current in neurons (I_{astro}). When a neuron fires, it releases quantal amounts of neurotransmitters (glutamate) into the synaptic cleft. Neurotransmitters bind to the

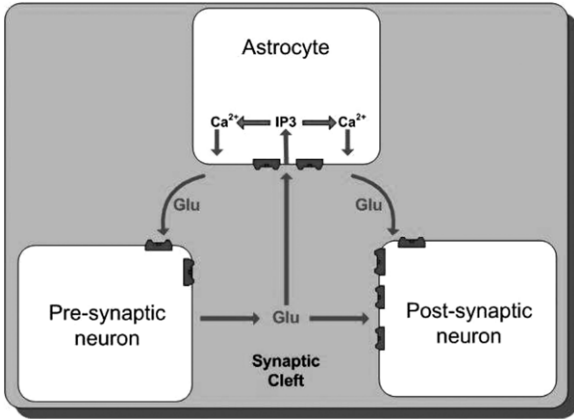


Fig. 1. Neuron–astrocyte interaction.

glutamate receptors on the astrocytes, triggering the release of intracellular IP3. The production of intracellular IP3 in the astrocyte can be assumed as quantized by the model of Nadkarni and Jung (Nadkarni & Jung, 2004):

$$\frac{d[\text{IP3}]}{dt} = \frac{1}{\tau_{\text{IP3}}} ([\text{IP3}]^* - [\text{IP3}]) + r_{\text{IP3}} \Theta(v - 50 \text{ mV}) \quad (4)$$

where $[\text{IP3}]^*$ is the equilibrium concentration of IP3. The parameter r_{IP3} determines the production of IP3 in response to a neuronal action potential. The production term is activated when the membrane potential v of the pre-synaptic neuron is larger than 50 mV via the Heaviside function Θ . Production of IP3, $[\text{IP3}]$, in the intracellular space of astrocytes triggers the calcium dynamics. The dynamics of intracellular calcium concentration $[\text{Ca}^{2+}]$ can be described according to LR model (Li & Rinzel, 1994):

$$\begin{cases} [\text{Ca}^{2+}]' = -J_{\text{chan}} - J_{\text{leak}} - J_{\text{pump}} \\ q' = \alpha_q(1 - q) - \beta_q q \end{cases} \quad (5)$$

where q is the fraction of activated IP3 receptor subunits. Calcium concentration is controlled by 3 fluxes, corresponding to:

$$J_{\text{leak}} = c_1 v_2 ([\text{Ca}^{2+}] - [\text{Ca}^{2+}]_{\text{ER}}) \quad (6)$$

$$J_{\text{pump}} = \frac{v_3 \cdot [\text{Ca}^{2+}]^2}{K_3^2 + [\text{Ca}^{2+}]^2} \quad (7)$$

$$J_{\text{chan}} = c_1 v_1 m_\infty^3 n_\infty^3 q^3 ([\text{Ca}^{2+}] - [\text{Ca}^{2+}]_{\text{ER}}) \quad (8)$$

where the gating/inactivation variables and their time-scales are given by:

$$m_\infty = \frac{[\text{IP3}]}{[\text{IP3}] + d_1} n_\infty = \frac{[\text{Ca}^{2+}]}{[\text{Ca}^{2+}] + d_5} \quad (9)$$

$$\alpha_q = a_2 d_2 \frac{[\text{IP3}] + d_1}{[\text{IP3}] + d_3} \beta_q = a_2 \cdot [\text{Ca}^{2+}] [\text{Ca}^{2+}]_{\text{ER}} = \frac{c_0 - [\text{Ca}^{2+}]}{c_1} \quad (10)$$

Nadkarni and Jung (Nadkarni & Jung, 2004) completed the model linking, by means of experimental data, the calcium concentration to the additional current toward the post-synaptic neuron (I_{astro}):

$$\begin{cases} I_{\text{astro}} = 2.11 \cdot \Theta[\ln(y)] \cdot \ln(y) \\ y = [\text{Ca}^{2+}] / nM - 196.69. \end{cases} \quad (11)$$

3. Neuron–astrocyte transistor-like model

We implemented and simulated the Nadkarni and Jung expressions and the LR model for pre-synaptic current, $I_n(t)$ and the r_{IP3}

Table 2
The parameters for LR model.

v_1	6 s^{-1}	d_1	$0.13 \text{ } \mu\text{M}$
v_2	0.11 s^{-1}	d_2	$1.049 \text{ } \mu\text{M}$
v_3	$0.9 \text{ } \mu\text{M} \cdot \text{s}^{-1}$	d_3	$0.9434 \text{ } \mu\text{M}$
C_0	$2 \text{ } \mu\text{M}$	d_5	$0.08234 \text{ } \mu\text{M}$
c_1	0.185	a_2	$0.2 \text{ } \mu\text{M}^{-1} \cdot \text{s}^{-1}$
K_3	$0.1 \text{ } \mu\text{M}$		

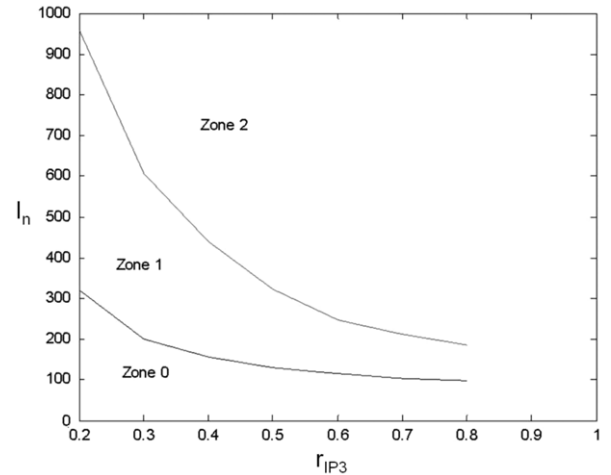


Fig. 2. Threshold curves identifying three separate $I_{\text{astro}}(t)$ behaviors.

Table 3
The fitting parameters of the thresholds.

	z_i (pA)	n_i	p_i
I_{th1}	78.59	-2.05	0.14
I_{th2}	136.07	-0.86	0.02

data. We adopted the original parameters used in the LR model (Table 2). By varying $I_n(t)$ and r_{IP3} , two curves (Fig. 2) identify three separate zones where three different $I_{\text{astro}}(t)$ behaviors are defined (Fig. 3).

The two threshold curves are identified using a fitting procedure based on Least-Mean-Square Algorithm (LMS Algorithm) as follows:

$$\begin{cases} I_{\text{th1}} = z_1 \cdot \sqrt[n_1]{r_{\text{IP3}} - p_1} \\ I_{\text{th2}} = z_2 \cdot \sqrt[n_2]{r_{\text{IP3}} - p_2}. \end{cases} \quad (12)$$

The fitting parameters are reported in Table 3.

In Zone 0 (Fig. 3(a)), when the neuron is stimulated the concentration of IP3 is not large enough to induce both calcium oscillations and $I_{\text{astro}}(t)$ values. In Zone 1 (Fig. 3(b)), the concentration of IP3 induces periodic waveforms both for calcium and $I_{\text{astro}}(t)$. In this case, $I_{\text{astro}}(t)$ consists of a rectified sinusoidal wave, i.e. the negative part of the wave is chopped. In addition, there is a variable delay between the start of the input current and the $I_{\text{astro}}(t)$ firing. In Zone 2 (Fig. 3(c)), both calcium curve and $I_{\text{astro}}(t)$ exhibit underdamped second order system-like behaviors, i.e. an overshoot and decaying oscillations approaching the final value. Also in this case, a variable delay between the start of the input current and the $I_{\text{astro}}(t)$ firing is induced. Reporting $I_{\text{astro}}(t)$ values versus r_{IP3} for different $I_n(t)$ input pre-synaptic currents (Fig. 4), we observe how $I_n(t)$ controls the $I_{\text{astro}}(t)$ flow likewise in a transistor the collector–emitter current can be viewed as being controlled by the base–emitter current.

Borrowing this concept, we can write I_{astro} in relation to the transfer function of the tripartite synapse, h_{syn} :

$$I_{\text{astro}}(t) = I_n(t) \cdot h_{\text{syn}}(t). \quad (13)$$

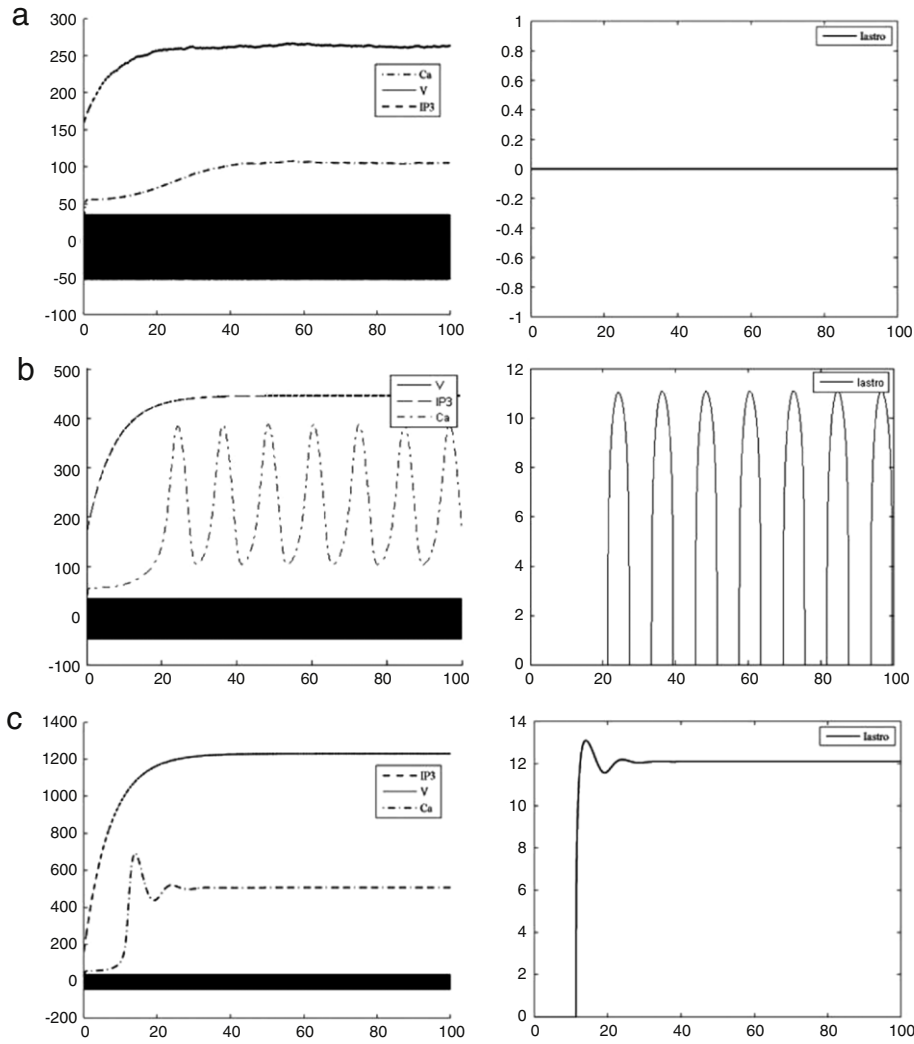


Fig. 3. Three $I_{astro}(t)$ behaviors with $I_n(t)$ and r_{IP3} in Zone 0, Zone 1 and Zone 2.

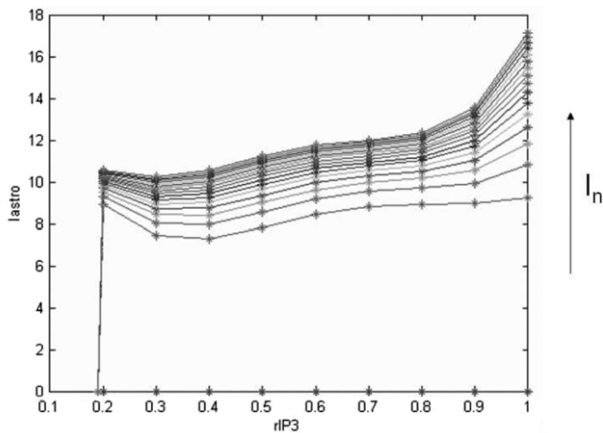


Fig. 4. $r_{IP3} - I_{astro}$ characteristics for various values of I_n .

In order to assess $h_{syn}(t)$, a fitting procedure for $I_{astro}(t)$ time course data obtained by Nadkarni and Jung and LR equations was carried out. The most suitable equations were the following:

$$h_{syn}(t) = \begin{cases} 0 & \text{if } I_n(t) \leq I_{th1} \\ \Theta(t - D_1) \cdot A_1 \cdot \sin(H) & \text{if } I_{th1} < I_n(t) \leq I_{th2} \\ \Theta(t - D_2) \cdot \frac{I_{astro}^* + A_2 \cdot e^{-\frac{t}{\tau}} \cdot \sin(2\pi f \cdot t)}{I_n} & \text{if } I_n(t) > I_{th2} \end{cases} \quad (14)$$

where time t is expressed in milliseconds and Θ is the Heaviside function.

In Zone 1, we calculated the following fitting relations:

$$\begin{cases} A_1 = \frac{k_3(I_n - I_{th1})^{k_4}}{I_n} \\ k_3 = a_{00} + a_{01}r_{IP3} + a_{02}r_{IP3}^2 + a_{03}r_{IP3}^3 + a_{04}r_{IP3}^4 \\ k_4 = a_{10} + a_{11}r_{IP3} + a_{12}r_{IP3}^2 + a_{13}r_{IP3}^3 + a_{14}r_{IP3}^4 \\ D_1 = a_{20} + a_{21}A_1 + a_{22}A_1^2 + a_{23}A_1^3 + a_{24}A_1^4. \end{cases} \quad (15)$$

The function H is the following triangular periodic waveform:

$$H = \begin{cases} \frac{\pi}{L \cdot T} \cdot t & \text{if } t \leq T_1 \\ 0 & \text{if } t > T_2 \end{cases} \quad (16)$$

where the triangular waveform period is $T = T_1 + T_2$ and:

$$\begin{cases} T = a_{30} + a_{31}A_1 + a_{32}A_1^2 \\ L = a_{40} + a_{41}A_1 + a_{42}A_1^2. \end{cases} \quad (17)$$

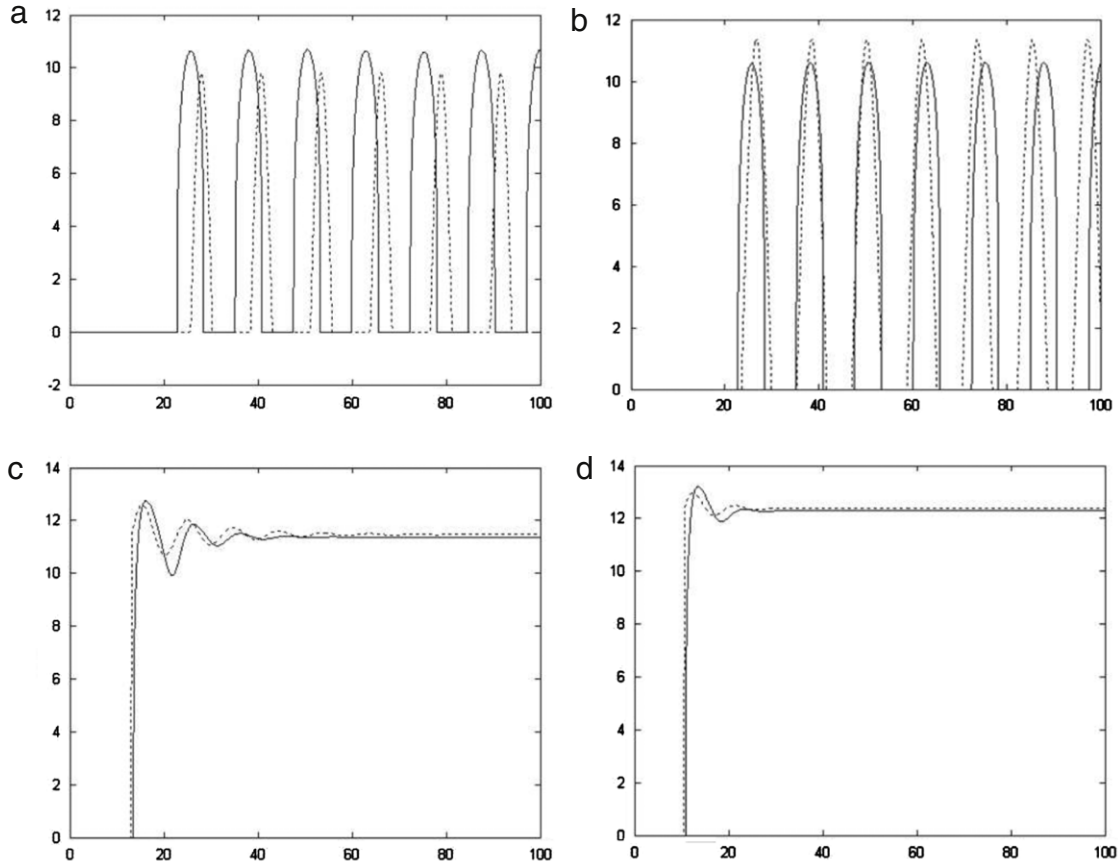


Fig. 5. Comparison between TLM (dotted line) and GSM (continuous line) in case of dc-current with (a) $I_n = 200$, $r_{IP3} = 0.4$, (b) $I_n = 600$, $r_{IP3} = 0.2$, (c) $I_n = 900$, $r_{IP3} = 0.4$, (d) $I_n = 900$, $r_{IP3} = 0.7$.

Table 4
Other fitting parameters.

a_{xy}	0	1	2	3	4
0	20.79	-105.7	257.04	-248.63	82.97
1	-0.20	1.94	-3.59	2.07	0
2	-2115.30	16 048.00	-3054.50	257.21	-8.56
3	2531.30	2502.60	-148.85	0	0
4	1.33	-0.28	0.01	0	0
5	3.48	33.48	-51.25	26.08	0
6	5.09×10^{-4}	1.18×10^{-3}	0	0	0
7	45 736.00	-2853.00	0	0	0
8	7.23	-0.51	0	0	0
9	6.98×10^{-3}	8.38×10^{-3}	0	0	0
10	1460.80	-234.40	9.43	0	0

In Zone 2, we calculated the following fitting relations:

$$\begin{cases} D_2 = a_{70} + a_{71}I_{astro}^* \\ A_2 = a_{80} + a_{81}I_{astro}^* \\ f = a_{90} + a_{91}I_{astro}^* \\ \tau = a_{100} + a_{101}I_{astro}^* + a_{102}I_{astro}^{*2} \end{cases} \quad (18)$$

where:

$$\begin{cases} I_{astro}^* = k_5 + k_6 I_n \\ k_5 = a_{50} + a_{51}r_{IP3} + a_{52}r_{IP3}^2 + a_{53}r_{IP3}^3 + a_{54}r_{IP3}^4 \\ k_6 = a_{60} + a_{61}r_{IP3} + a_{62}r_{IP3}^2 + a_{63}r_{IP3}^3 + a_{64}r_{IP3}^4. \end{cases} \quad (19)$$

The fitting parameters are reported in Table 4.

Since several variables, e.g. I_{astro}^* and A_1 , are function of the time-dependent $I_n(t)$, a re-calculation of the model parameters is required for each millisecond of simulation. Here, we report on results on modeling the simplest possible neural–glial circuit,

Table 5
Comparison between the two simulated dressed neuron with dc-current as input.

Zone (pA)	$r_{IP3} 0.2$	$r_{IP3} 0.3$	$r_{IP3} 0.4$	$r_{IP3} 0.5$	$r_{IP3} 0.6$	$r_{IP3} 0.7$	$r_{IP3} 0.8$
$I_n = 100$	0	0	0	0	0	0	1**
$I_n = 200$	0	1*	1*	1**	1**	1**	2**
$I_n = 300$	0	1**	1**	1**	2**	2**	2**
$I_n = 400$	0	1**	1**	2**	2**	2**	2**
$I_n = 500$	1**	1**	2**	2**	2**	2**	2**
$I_n = 600$	1**	1**	2**	2**	2**	2**	2**
$I_n = 700$	1*	2**	2**	2**	2**	2**	2**
$I_n = 800$	1**	2**	2**	2**	2**	2**	2**
$I_n = 900$	1**	2**	2**	2**	2**	2**	2**
$I_n = 1000$	2**	2**	2**	2**	2**	2**	2**
$I_n = 1100$	2**	2**	2**	2**	2**	2**	2**
$I_n = 1200$	2**	2**	2**	2**	2**	2**	2**

* $p < 0.005$.
** $p < 0.0001$.

i.e. a single neuron, stimulated by a dc-current and ac-current, coupled to an astrocyte. Two dressed neurons were implemented. In the former, the Gold Standard Model (GSM), the RS neuron was modeled by the Izhikevich formulation and the neuron–astrocyte interactions by Nadkarni and Jung and the LR expressions. In the latter, the proposed Transistor-Like Model (TLM), the neuron was modeled by the Izhikevich formulation and the neuron–astrocyte interactions by our transistor-like relationships. We tested both the dressed neurons by injecting input currents, $I_n(t)$, to the neuron in the range 100–1200 pA for 100 s with 1 ms of time resolution.

In the Table 5 results from GSM and TLM simulations by using dc-current are showed; for each row and column the zone in which different $I_{astro}(t)$ behaviors were found is reported. The p -value calculation was performed by means of the Pearson correlation

Table 6
Comparison between the two simulated dressed neuron with ac-current as input.

Zone	$r_{IP_3} 0.2$	$r_{IP_3} 0.3$	$r_{IP_3} 0.4$	$r_{IP_3} 0.5$	$r_{IP_3} 0.6$	$r_{IP_3} 0.7$	$r_{IP_3} 0.8$
$M = 100 \text{ pA}, f_0 = 0.1 \text{ Hz}$	0	0	0	0	0	0	NaN
$M = 200 \text{ pA}, f_0 = 0.1 \text{ Hz}$	0	NaN	1*	1**	NaN	1**	1**
$M = 300 \text{ pA}, f_0 = 0.1 \text{ Hz}$	0	1*	NaN	1**	1**	2**	2**
$M = 400 \text{ pA}, f_0 = 0.1 \text{ Hz}$	1**	1**	1**	1**	2**	2**	2**
$M = 500 \text{ pA}, f_0 = 0.1 \text{ Hz}$	1**	1*	1**	2**	2**	2**	2**
$M = 600 \text{ pA}, f_0 = 0.1 \text{ Hz}$	1*	NaN	2**	2**	2**	2**	2**
$M = 700 \text{ pA}, f_0 = 0.1 \text{ Hz}$	1**	1**	2**	2**	2**	2**	2**
$M = 800 \text{ pA}, f_0 = 0.1 \text{ Hz}$	1**	2**	2**	2**	2**	2**	2**
$M = 900 \text{ pA}, f_0 = 0.1 \text{ Hz}$	1*	2**	2**	2**	2**	2**	2**
$M = 1000 \text{ pA}, f_0 = 0.1 \text{ Hz}$	2**	2**	2**	2**	2**	2**	2**
$M = 1100 \text{ pA}, f_0 = 0.1 \text{ Hz}$	2**	2**	2**	2**	2**	2**	2**
$M = 1200 \text{ pA}, f_0 = 0.1 \text{ Hz}$	2**	2**	2**	2**	2**	2**	2**

* $p < 0.005$.

** $p < 0.0001$.

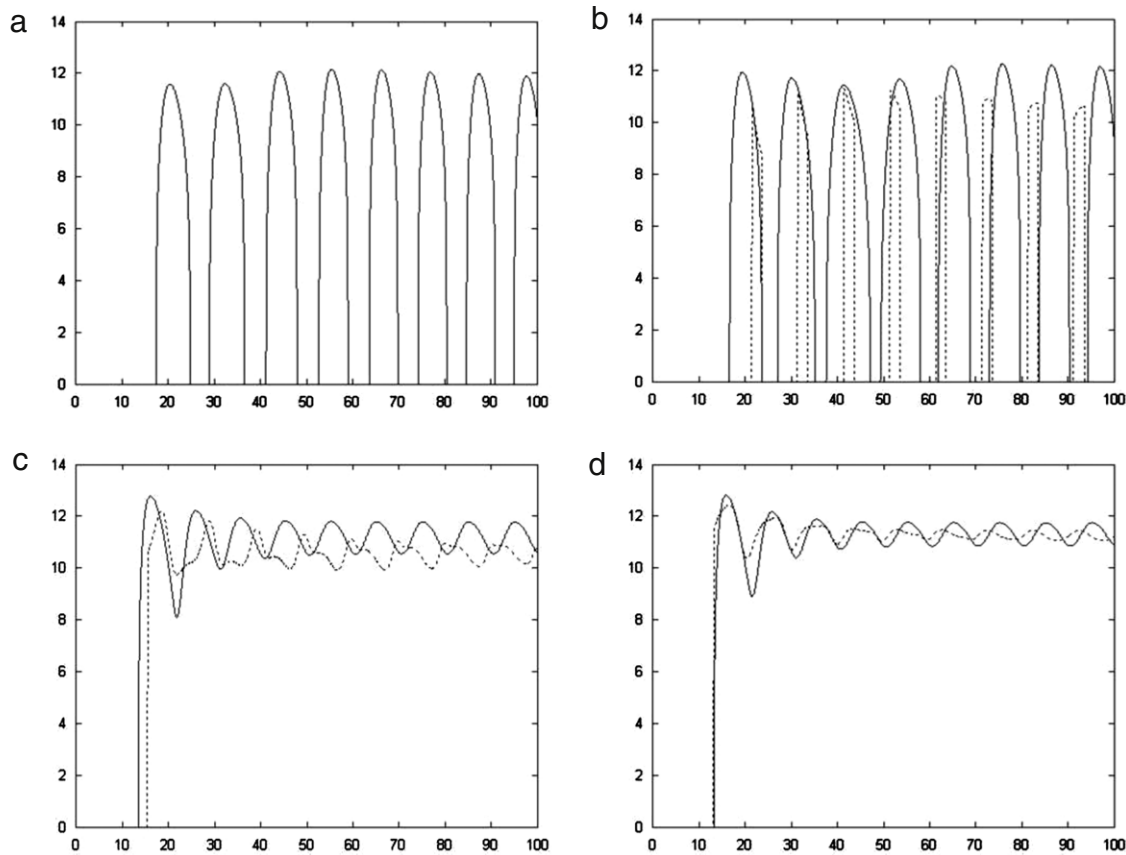


Fig. 6. Comparison between TLM (dotted line) and GSM (continuous line) in case of ac-current with (a) $M = 200, r_{IP_3} = 0.6$, (b) $M = 500, r_{IP_3} = 0.3$, (c) $M = 1000, r_{IP_3} = 0.3$, (d) $M = 700, r_{IP_3} = 0.4$.

coefficient. Moreover, results from GSM and TLM simulations by using ac-current were also calculated (Table 6). We chose a time variant signal having sinusoidal shape as following:

$$I_n(t) = M + \frac{M}{4} \sin(2\pi f_0 t). \quad (20)$$

According to dc-current findings, the output of the considered models show good statistical significance as well. Some cases, labeled as *NaN*, presented different behavior between GSM and TLM output. The simulation results regarding the transistor-like model are in agreement with the ones obtained by the Nadkarni and Jung and the LR expressions. Examples of the two dressed neurons model output having different statistical significance are shown in Figs. 5 and 6.

4. Conclusions

In this article, we described the dressed neuron signaling through a nonlinear transistor-like transfer function. We derived the astrocytic current in function of both the pre-synaptic neuron current and the r_{IP_3} of the astrocyte starting from computational data obtained implementing existing biophysical neuron–glia models (LR model). This work represents a computationally efficient model describing the synapse and astrocyte couplings. Through the model here proposed, indeed, it is possible to simulate real-time spiking artificial neuron–glia networks realizing the mechanism which seems to be a necessary part of the regulation of spiking activities. We demonstrated that this model is suitable to simulate the neuron–astrocyte signaling phenomena.

References

- Allegrini, P., Fronzoni, L., Pirino, , & Pirino, D. (2009). The influence of the astrocyte field on neural dynamics and synchronization. *Journal of Biological Physics*.
- De Pitta, M., Goldberg, M., Volman, V., Berry, H., & Ben-Jacob, E. (2009). Glutamate regulation of calcium and IP3 oscillating and pulsating dynamics in astrocytes. *Journal of Biological Physics*.
- De Pitta, M., Volman, V., Levine, G., Pioggia, D., De Rossi, D., & Ben-Jacob, E. (2008). Coexistence of amplitude and frequency modulations in intracellular calcium dynamics. *Physical Review E*, 77, 030903(R).
- Di Garbo, A., Barbi, M., Chillemi, S., Alloisio, S., & Nobile, M. (2007). Calcium signalling in astrocytes and modulation of neural activity. *BioSystems*, 89, 74–83.
- Fellin, T., & Carmignoto, G. (2004). Neuron-to-astrocyte signalling in the brain represents a distinct multifunctional unit. *Neural Computation*, 16(1), 3–15.
- FitzHugh, R. (1961). Impulse and physiological states in models of nerve membrane. *Biophysical Journal*, 1(6), 445–466.
- Hodgkin, & Huxley, (1952). A quantitative description of membrane current and its application to conduction and excitation in nerve. *Journal of Physiology*, 117, 500–544.
- Izhikevich, E. M. (2003). Simple model of spiking neurons. *IEEE Transactions on Neural Networks*, 15(5), 1569–1572.
- Izhikevich, E. M. (2004). Which model to use for cortical spiking neurons? *IEEE Transactions on Neural Networks*, 15(6), 1063–1070.
- Izhikevich, E. M. (2007). *Dynamical systems in neuroscience: the geometry of excitability and bursting*. The MIT press.
- Li, X. Y., & Rinzel, J. (1994). Equations of IP3 receptor-mediated Ca2+ oscillations derived from a detailed kinetic model: a Hodgkin–Huxley like formalism. *Journal of Theoretical Biology*, 166, 461–473.
- Morris, C., & Lecar, H. (1981). Voltage oscillations in the barnacle giant muscle fiber. *Biophysical Journal*, 35(1), 193–213.
- Nadkarni, S., & Jung, P. (2004). Dressed neurons: modelling neural-glia interactions. *Physical Biology*, 1, 35–41.
- Nadkarni, S., & Jung, P. (2003). Spontaneous oscillations of dressed neurons: a new mechanism for epilepsy? *Physical Review Letters*, 91(4), 268101.
- Newman, E. A. (2003). New roles for astrocytes: regulation of synaptic transmission. *Trends in Neurosciences*, 26, 536–542.
- Nobile, M., Monaldi, I., Alloisio, S., Cugnoli, C., & Ferroni, S. (2003). ATP-induced, sustained signalling in cultured rat cortical astrocytes: evidence for a non-capacitive, P2X7-like-mediated calcium entry/Glutamate-mediate astrocyte-neuron signalling. *FEBS Letters*, 538, 71–76.
- Parpura, V., Basarsky, T. A., Liu, F., Jeftinija, K., Jeftinija, S., & Haydon, P. G. (1994). Glutamate-mediate astrocyte-neuron signalling. *Nature*, 369, 744–747.
- Parpura, V., & Haydon, P. G. (2000). Physiological astrocytic calcium levels stimulate glutamate release to modulate adjacent neurons. *Proceedings of the National Academy of Sciences USA*, 97, 8629–8634.
- Volman, V., Ben-Jacob, E., & Levine, H. (2007). The astrocyte as a gatekeeper of synaptic information transfer. *Neural Computation*, 19, 303–326.